JOURNAL OF APPLIED CRYSTALLOGRAPHY

**Volume 53 (2020)**

**Supporting information for article:**

# *In situ* temperature profile measurements with high-energy X-rays as a probe of optical floating zone crystal-growth environment

**Jonathan J. Denney, Yusu Wang, Adam A. Corrao, Guanglong Huang, David Montiel, Hui Zhong, Eric Dooryhee, Katsuyo Thornton and Peter G. Khalifah**

## S1. Geometry of diffraction experiments

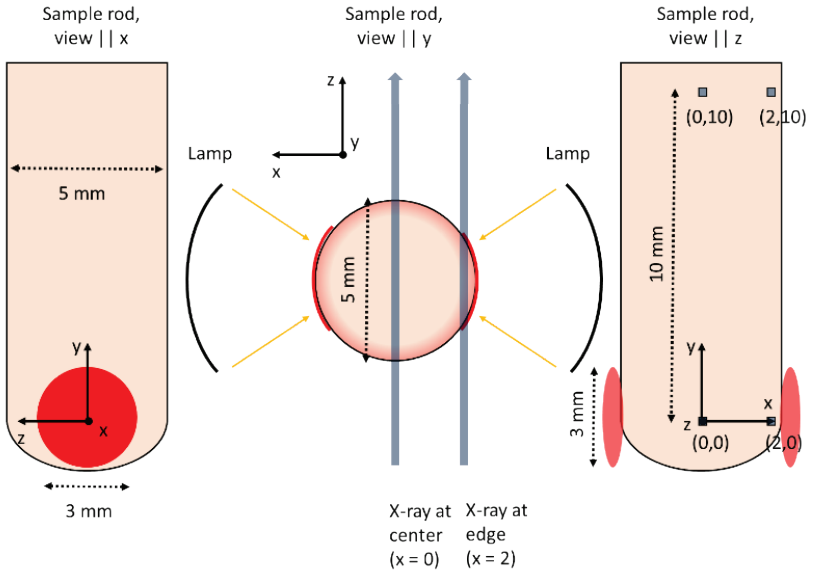


**Figure S1** Geometry and coordinate system for diffraction experiments, shown approximately to scale as viewed from the direction of the x-axis (left), y-axis (center), and z-axis (right). The rod (~5 mm diameter) is shown in tan while the focal spots of the lamps (~3 mm diameter) are shown in red. Although the lamp focal spots are drawn on the surface of this image, in reality the alignment was carried out so that the lamps (19 mm focal length) are focused to the center of the rod, so the spot diameter on the surface should be slightly larger than 3 mm. The X-ray beam (blue, parallel to *z*) has a square cross-section, which is shown approximately to scale in the right panel. Similarly, the width of the beam relative to the sample is also approximately to scale in the center panel.

As can be seen from the schematic of the experiment geometry (Figure S1, center), diffraction experiments were carried out in a transmission geometry. The path length at the center position ($x$ = 0) is equal to the rod diameter (~5 mm), while the path length at the edge position ($x$ = 2.075 mm) will be about 56% of that length. If there is a center-to-edge temperature gradient (schematically represented by the darker ring around the circumference in the center panel), the temperature determined by diffraction for the edge position will fairly accurately represent the edge temperature while the temperature determined for the center position will instead represent a weighted average between the center and the edge temperature. As such, these methods will be effective for resolving the presence or absence of a temperature gradient but will not permit the direct determination of the center temperature. Alternative diffraction methods with 3D sensitivity (such as diffraction tomography) may be more effective at providing this information. All temperatures obtained through simulations (*e.g.*, Figure 7) were averaged along the *z*-axis to permit direct comparisons with experimental data.

**S2. Representative data**

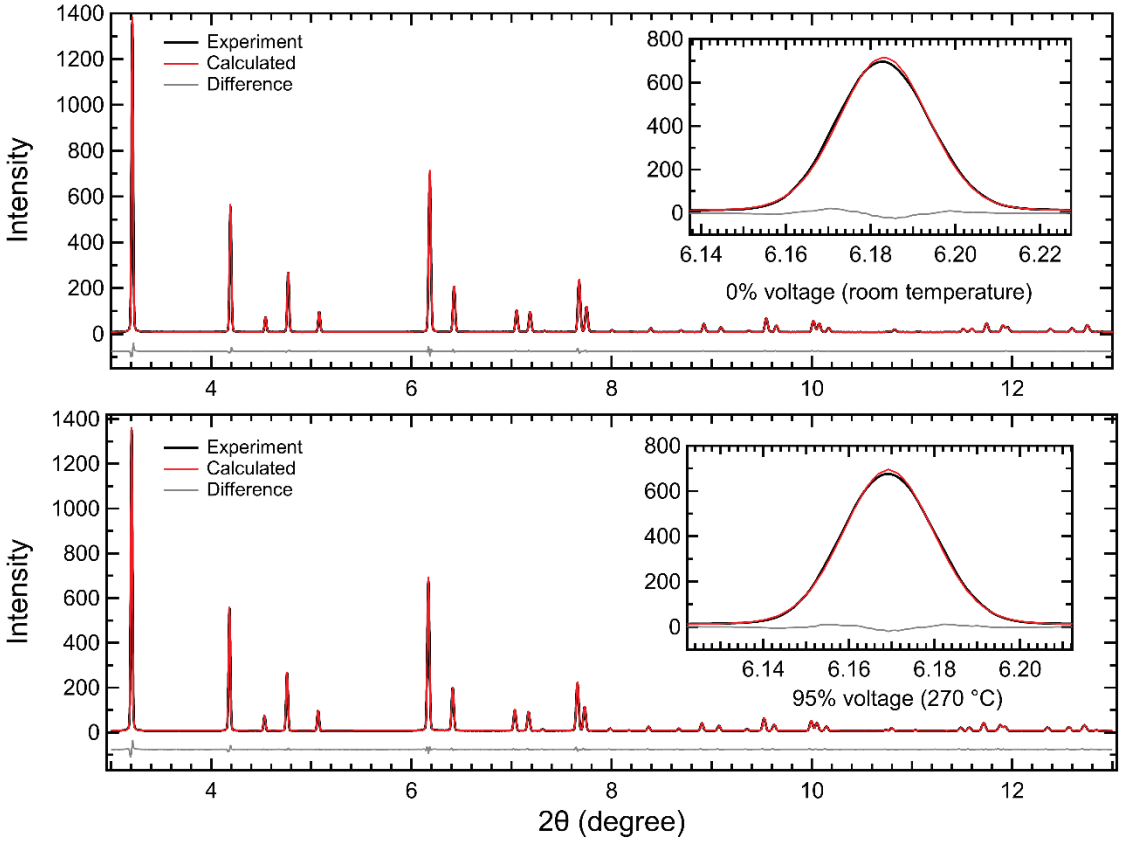


**Figure S2** Pawley fits to representative data collected at room temperature (top) and after equilibration at maximum power (bottom). Data are shown in black, the calculated pattern in red, and the difference pattern in gray. For clarity, the difference patterns are given a vertical offset of -75 in the main panels (but not the insets). The raw data and control files for the Pawley fits are provided as online Supporting Information.

### S3. Design of mini-FZ furnace

The general goal of the mini-FZ furnace is to allow the point heating of a polycrystalline rod to high temperatures using lamps as the power source while maintaining a clear entry and exit path for an X-ray beam, allowing temperature profiles to be measured via the translation of the entire sample/furnace assembly (both mounted on a single stiff steel baseplate, Part #18).

### S3.1. Design of Mark II mini-FZ furnace

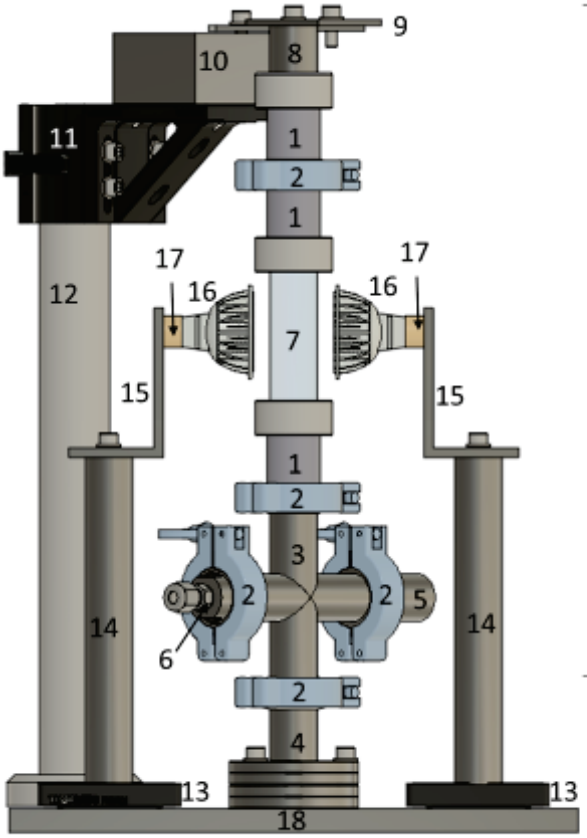


| Number | Quantity | Description |
|---|---|---|
| 1 | 3 | KF25 to Quick-Connect Couplings (Steel) 1" tube diameter |
| 2 | 5 | KF25 Cast Clamps (Aluminum) |
| 3 | 1 | 4-Way KF25 Cross (Steel) |
| 4 | 1 | CF35 to KF25 Adapter Flange (Steel) and Fixed Tapped-Blank CF35 Flange (Steel) |
| 5 | 1 | KF25 Half Nipple (Steel) |
| 6 | 1 | KF25 to ¼" Female NPT Adapter (Steel) and Swagelok to ¼" Male NPT Adapter (Steel) |
| 7 | 1 | Quartz glass tube 1" OD |
| 8 | 1 | Sample mounting rod 1" OD 3" L (Aluminum) |
| 9 | 1 | Chamber Stabilizing bracket (Steel) |
| 10 | 1 | Threaded Spacer (Steel) |
| 11 | 1 | Mounting Clamp (Steel) |
| 12 | 1 | Support Rod 1.5" OD 14"L (Steel) |
| 13 | 2 | Magnetic Base clamps |
| 14 | 2 | Lamp Spacers 1' OD 7" L (Aluminum) |
| 15 | 2 | Lamp angle brackets (Aluminum) |
| 16 | 2 | MR16 Halogen Lamps with gold reflectors |
| 17 | 2 | Sockets |
| 18 | 1 | Baseplate 6' L 12' W (Steel) |

**Figure S3** Schematic of Mark II mini-FZ furnace design

The more complex Mark II mini-FZ furnace will be described first. It consists of three main parts: a lower section providing environmental control (Parts 1 – 7) connected to an upper section holding the sample rod in place (Parts 8 – 12) as well as a mounting system for 150 W halogen lamps in a gold-coated mirror housing (Parts 13 – 17). A schematic of this furnace is provided together with a list of parts in Figure S1. The sample rod was attached to an alumina mounting bracket purchased as part of a commercial floating zone furnace (Crystal Systems Corporation) using three wires; this bracket was then threaded into a matching hole tapped into the lower face of Part 8. The two furnace lamps (Oriel, MR16) were connected in series, with power provided using an external power supply with output voltage control. The positions of the lamps were individually adjusted manually and then fixed in place using the locking magnetic bases.

The chamber could be evacuated using the integral hose fitting (Part 5) which was connected to a vacuum pump by way of a T-fitting that contained connections for (1) a manual pressure gauge and (2) an oil bubbler behind a shut-off valve that allowed the system to be safely back-filled with gas after evacuation. The back-filled gas was introduced through an integral Swagelok fitting (Part 6) using a gas line that contained a pressure relief check valve to prevent accidental over-pressurization of the system.

The alignment of the upper and lower portions of the sample environment was facilitated using a swing arm consisting of two metal plates held together with a nut and bolt (Part 9), allowing a fused silica tube (Part 7) to provide environmental control while still allowing the lamps to effectively heat the sample. The baseplate holding the furnace and sample assembly was connected to the upper M6 mounting grid of the PDF beamline using of two adjustable struts that could be bolted to the baseplate, allowing the entire assembly to move through motorized *xyz* position changes.

### S3.2. Design of Mark I mini-FZ furnace

The Mark I furnace was a simpler design constructed for initial proof-of-principle experiments. The lamp design was essentially the same though shorter mounting rods (Part 14) were utilized. The upper sample holder had a different design - Part 8 was replaced with a small goniometer head (Huber, 1007-S) to which the sample mounting bracket was attached using the integral set screw. The environmental control portions (Parts 1 – 7) were not included in this design except for a single compression fitting (Part 1) that could serve to safely catch any material (molten or powder) falling from the sample rod. This compression fitting was used without any tube in the experiments described here.

### S3.3. Alignment procedures

The design of the Mark I and Mark II furnaces did not permit the precise alignment of lamps and of the sample rod. Lamps were positioned by hand (using a ruler) so that the front of reflector frames were 38 mm apart, so that the manufacturer-specified focal spots of the lamp (19 mm from front of frame) would coincide with each other. The ceramic rods were also aligned by hand. Since the rods were not perfectly straight, and since the limited accessible sample space between the lamp made measurements difficult, the precision of alignment was low. Direct measurements of alignment errors were impossible; alignment errors of 1 mm or more were certainly possible and are the likely origin of the horizontal gradients seen in Figure 4.

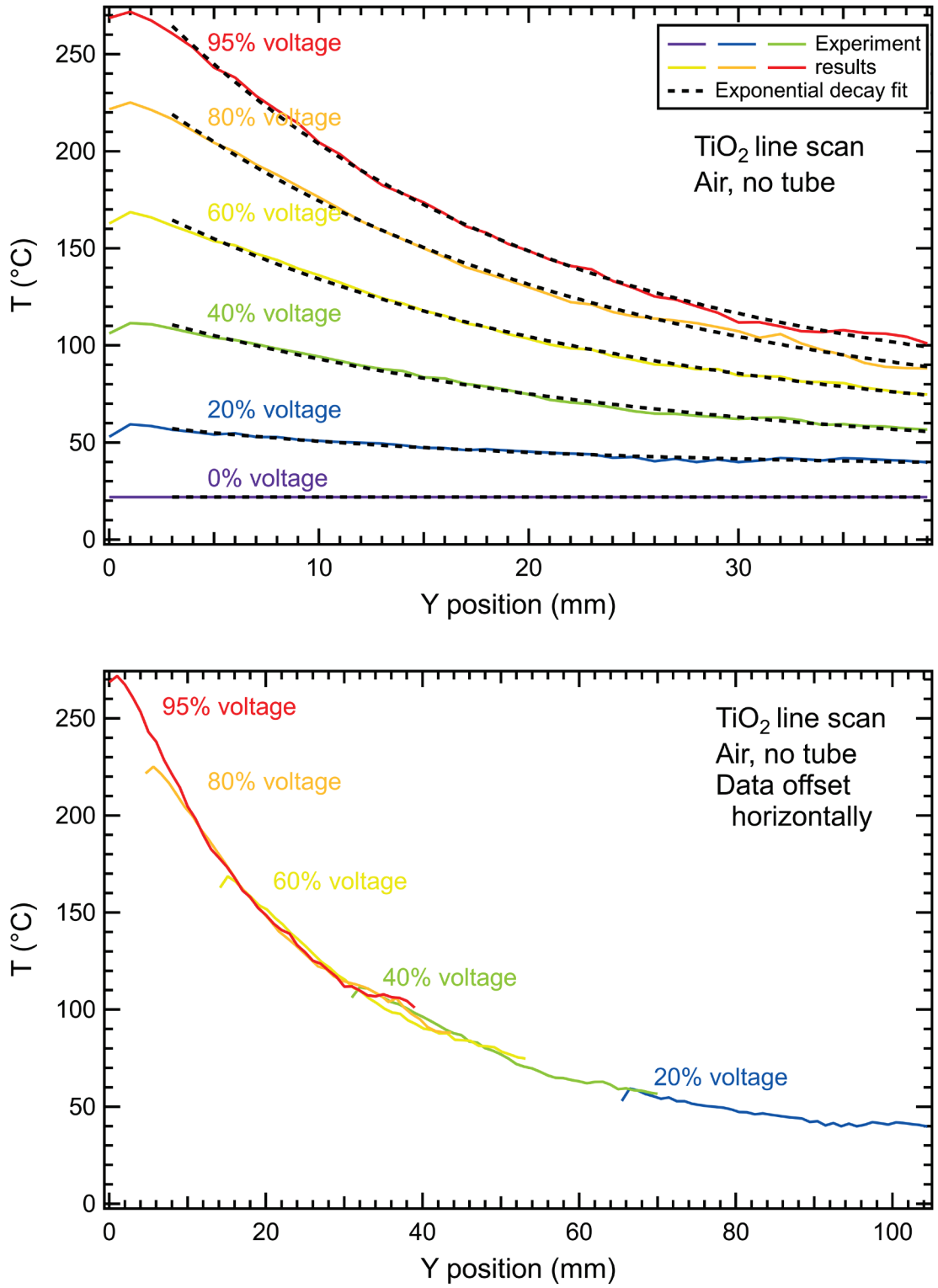


**Figure S4** (Top) Fits of experimentally determined temperature profile along the $TiO_2$ rod at different power levels to an exponential decay functional form. Although this functional form is not strictly correct, it effectively reproduces observed results. (Bottom) The same data can be overlaid on a common curve using only horizontal offsets, indicating that equivalent heat transfer mechanisms are operative at all power levels.

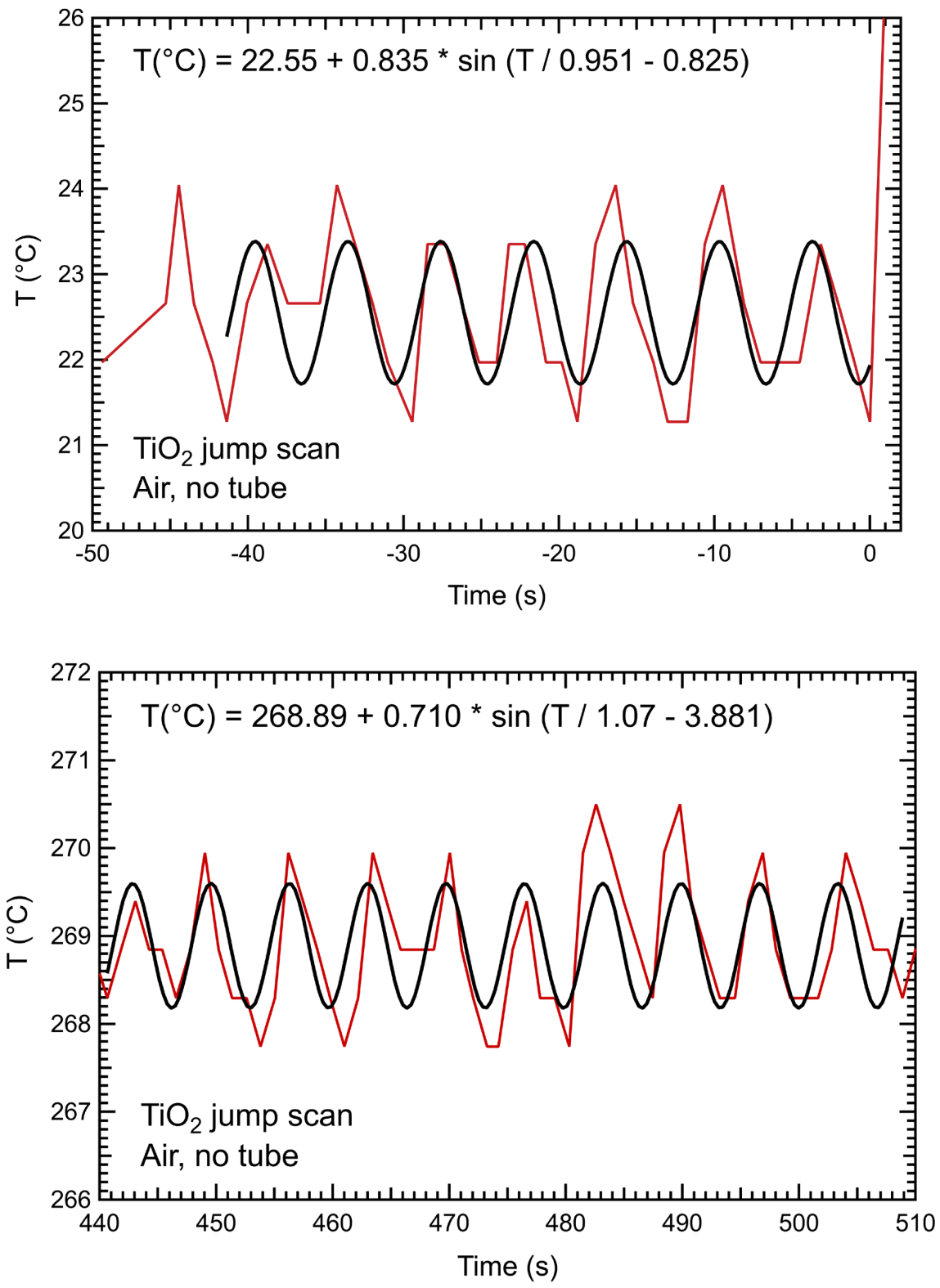


**Figure S5** Fluctuations in nominal temperature (red) observed at room temperature before heating (top) and at elevated temperature after equilibration for a power jump time series to 95% power (bottom) for the data collected at the bottom (z = 0 mm) center position of the rod. Fits to a sinusoidal oscillation with the equation specified in the legend are overlaid as a black line on top of experimental data (red line).

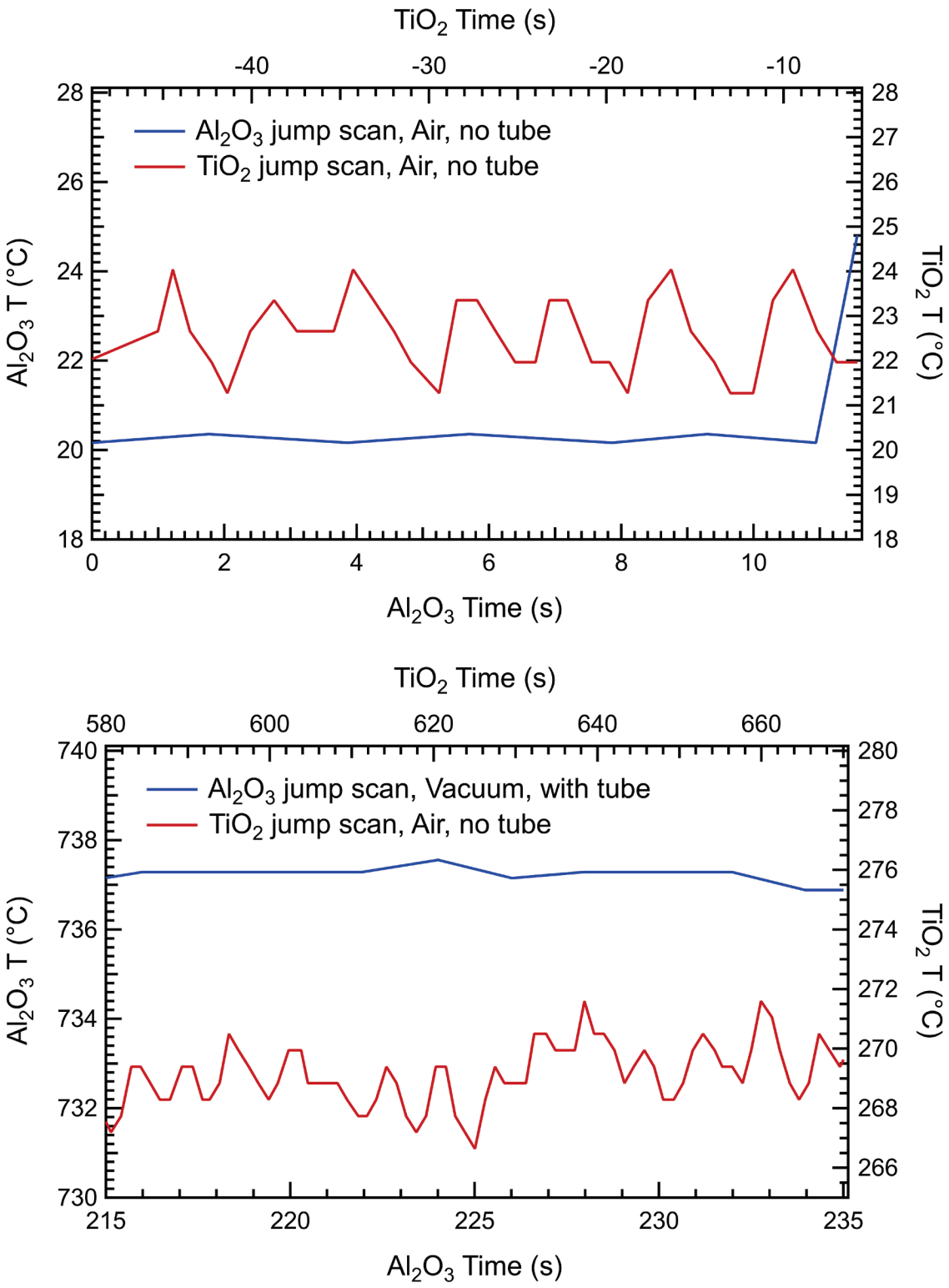


**Figure S6** Comparison of equilibrium temperature fluctuations (blue) before the start of heating (top) and after equilibration (bottom) after a temperature jump for an $Al_2O_3$ rod in the Mark II furnace (blue) and for a $TiO_2$ rod in the Mark I furnace (red). The periodic vibrations affecting the Mark I furnace (red) were not observed for the Mark II, which showed a temperature stability of better than ±0.25 °C, corresponding to fluctuations in the refined unit cell volume of less than 0.001 Å$^3$.

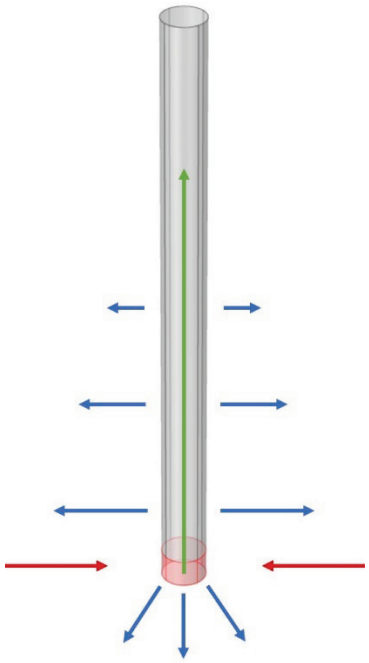

**Figure S7** Thermal processes in heated rods that affect the temperature profile include (1) applied heat from lamps (red) which deposits heat in a narrow region near the tip of the sample, (2) thermal transport through polycrystalline rod (green arrow) away from the hot zone, and (3) heat loss from the rod surface (blue arrows), which occurs through a combination of gray body radiation and thermal conduction of the surrounding atmosphere.

**Table S1** Comparison of experimental lamp power and modeled heating power.

| Voltage (%) | Lamp power[1] (W) | Heating power (W) |
|---|---|---|
| 20 | 25.2 | 0.27 |
| 40 | 72.96 | 0.7875 |
| 60 | 137.16 | 1.35 |
| 80 | 215.52 | 2.0025 |
| 95 | 282.15 | 2.52 |

[1]Lamp power was calculated based on the recorded current and voltage from the power supply ($P = IV$) assuming zero resistance in the wires connecting the power supply to the lamp.

**Table S2** Voltage, current, resistance, and power based off power supply

| Voltage (V) | Current (A) | Resistance (Ω) | Power (W) |
|---|---|---|---|
| 6.03 | 4.15 | 1.45 | 25.0 |
| 12.05 | 6.04 | 1.99 | 72.8 |
| 15.05 | 6.95 | 2.16 | 105 |
| 18.07 | 7.58 | 2.38 | 137 |
| 24.07 | 8.94 | 2.69 | 215 |
| 28.56 | 9.87 | 2.89 | 282 |
| 29.97 | 9.98 | 3.00 | 299 |

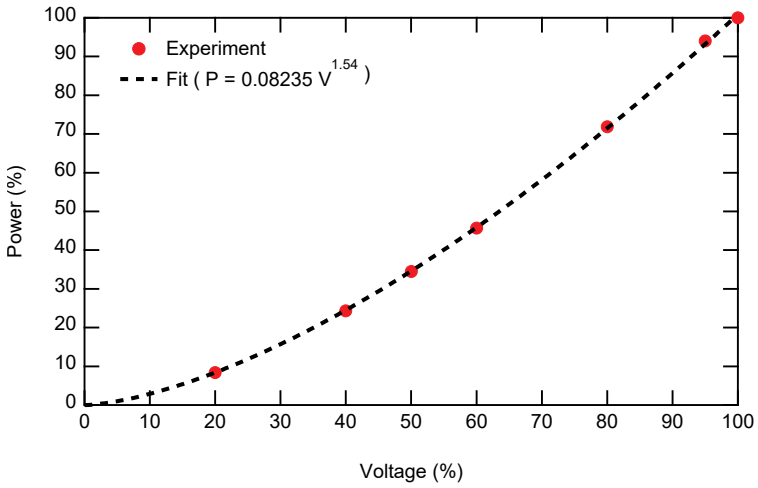


**Figure S8** Relationship between set voltage and electrical power applied to lamps.